AMPK and GCN2-ATF4 signal the repression of mitochondria in colon cancer cells

Inmaculada Martínez-Reyes, María Sánchez-Aragó and José M. Cuezva*

Departamento de Biología Molecular, Centro de Biología Molecular Severo Ochoa, Consejo Superior de Investigaciones Científicas-Universidad Autónoma de Madrid (CSIC-UAM), Centro de Investigación Biomédica en Red de Enfermedades Raras CIBERER-ISCIII, Instituto de Investigación Hospital 12 de Octubre, Universidad Autónoma de Madrid, 28049 Madrid, Spain.

Short title: Signaling the metabolic switch of tumor promotion

Keywords: ATP synthase; Cancer; Cellular stress; Glycolysis; Mitochondria; Translational control.

*, To whom correspondence should be address to:
Prof. José M. Cuezva,
Centro de Biología Molecular Severo Ochoa,
Universidad Autónoma de Madrid, 28049 Madrid, Spain.
Phone: 34-91 196 4618;
Fax: 34-91 196 4420;
E-mail: jmcuezva@cbm.uam.es

Abbreviations: β-F1-ATPase, β catalytic subunit of the mitochondrial H^+-ATP synthase; GAPDH, glyceraldehyde-3-phosphate dehydrogenase; Hsp60, heat–shock protein 60; OL, oligomycin; PBS, phosphate-buffered saline; α F1-ATPase, α catalytic subunit of the mitochondrial H^+-ATP synthase; PK, pyruvate kinase; FBS, fetal bovine serum; AICAR, 5-aminoimidazole-4-carboxamide 1-β-D-ribofuranoside; SDHA, succinate dehydrogenase subunit A; PDH, pyruvate dehydrogenase; COX I, cytochrome c oxidase subunit I; COX IV, cytochrome c oxidase subunit IV; HIF1 α, hypoxia inducible factor 1 alpha subunit; GRK2, G protein-coupled receptor kinase 2; PGC1 α, peroxisome proliferator-activated receptor gamma coactivator 1 alpha; Akt, v-akt murine thymoma viral oncogene; AMPK, protein kinase, AMP-activated; p38 MAPK, mitogen-activated protein kinase 14; mTOR, mammalian target of rapamycin (serine/threonine kinase); 4EBP1, eukaryotic translation initiation factor 4E binding protein 1; p70S6K, ribosomal protein S6 kinase, 70kDa, polypeptide 1; HuR, ELAV-like protein; GCN2, eukaryotic translation initiation factor 2-alpha kinase; eIF2 α, eukaryotic translation initiation factor 2 subunit A; ATF4, activating transcription factor 4; LC3, microtubule-associated protein 1 light chain 3 alpha; raptor, regulatory-associated protein of mTOR; S6, ribosomal protein S6; ACC, acetyl-CoA carboxylase; ULK1, unc-51-like kinase 1; p62, sequestosome 1.

SYNOPSIS

Reprogramming of energetic metabolism is a phenotypic trait of cancer in which mitochondrial dysfunction represents a key event in tumor progression. Herein, we show that the acquisition of the tumor promoting phenotype in colon cancer HCT116 cells treated with oligomycin to inhibit the ATP synthase is exerted by repression of the synthesis of nuclear-encoded mitochondrial proteins in a process that is regulated at the level of translation. Remarkably, the synthesis of glycolytic proteins is not affected in this situation. Changes in translational control of mitochondrial proteins are signaled by the activation of AMP-activated protein kinase (AMPK) and the General Control nondepresible-2 (GCN2) kinase, leading also to the activation of autophagy. Changes in the bioenergetic function of mitochondria are mimicked by the activation of AMPK and the silencing of Activating Transcription Factor 4 (ATF4). These findings emphasize the relevance of translational control for normal mitochondrial function and for the progression of cancer. Moreover, demonstrate that glycolysis and oxidative phosphorylation are controlled at different levels of gene expression, offering to the cell a mechanistic safeguard strategy for metabolic adaptation under stressful conditions.

INTRODUCTION

Mitochondria play a central role in the homeostasis of higher eukaryotic cells. The provision of metabolic energy by oxidative phosphorylation, the execution of cell death and intracellular signaling by Ca^{2+} and reactive oxygen species (ROS) are main cellular functions of the organelle. A growing number of human diseases, which include cancer, are associated with the molecular and/or functional alteration of mitochondria [1, 2]. The biogenesis of mitochondria is a complex genetic program that requires the concerted transcriptional response of nuclear and mitochondrial genes [3]. However, mechanisms that control the localization and translation of mRNAs also contribute to define the mitochondrial phenotype of the cell, offering the biogenesis of the H^+-ATP synthase a paradigm in this regard [4]. Indeed, a master regulator in the provision of metabolic energy by oxidative phosphorylation is the mitochondrial H^+-ATP synthase, a rotatory engine that utilizes the proton electrochemical gradient generated by the respiratory chain as a driving force for the phosphorylation of ADP [5].

Cancer is a complex genetic disease in which the tumor microenvironment plays a fundamental role for disease progression [6, 7]. A hallmark of cancer cells and tumors is its peculiar energy metabolism [1, 8]. Carcinomas display increased glucose consumption rates due to a low activity of oxidative phosphorylation, concurrently showing higher rates of lactate production when compared to normal tissues [9]. It has been consistently reported that the relative expression of β-F1-ATPase[1] (β catalytic subunit of the mitochondrial H^+-ATP synthase), which is the catalytic subunit of the H^+-ATP synthase, is significantly diminished in tumors when compared to its expression in normal tissues [1, 10]. In a large number of different carcinomas the down-regulation of β-F1-ATPase is accompanied by an increased expression of markers of the glycolytic pathway [1, 10]. This proteomic feature of cancer defines a "bioenergetic signature" of clinical relevance as an indicator of disease progression in colon, lung and breast cancer patients (for reviews see [1, 4]) as well as a predictive marker of the cellular response to chemotherapy [1, 11, 12]. Remarkably, recent findings have demonstrated that the activity of the H^+-ATP synthase itself is inhibited in human carcinomas by up-regulation of its physiological inhibitor IF1, which is a relevant regulator of energetic metabolism in cancer cells [13]. The expression of β-F1-ATPase in developing liver [14, 15], brown adipose tissue [16], during progression through the cell cycle [17] and in rat [18] and human [19] carcinomas is exerted at the level of translation and largely mediated by the 3'UTR of the mRNA [14, 18, 19]. Similar findings have been obtained in yeast, where deletion of the 3'UTR leads to reduced ATP synthesis and respiratory dysfunction [20]. In addition, RNA binding proteins (RNABPs) of β-F1-ATPase mRNA (β-mRNA) have been shown to exert a relevant role in the control of translation of the mRNA both in development [14] and in carcinogenesis [18, 21].

Down-regulation of β-F1-ATPase and the suppression of the bioenergetic activity of mitochondria is a required event to promote *in vivo* tumor progression in colon cancer [22]. In fact, we have recently demonstrated [22] that tumor xenografts derived from three isogenic HCT116 colon cancer cell lines differing in the expression level of β-F1-ATPase only develop when cells with the highly glycolytic phenotype are selected, i.e., tumor development requires the selection of cancer cells with a repressed biogenesis and functional activity of mitochondria. In other words, cancer cells with a functional activity of mitochondria are unable to develop tumors [22]. Importantly, such tumors displayed the transcriptomic, proteomic and mitochondrial ultrastructure of the cells treated with oligomycin [22]. These findings strongly emphasized the relevance of the cancer cell microenvironment for tumor

progression, further suggesting that cells treated with oligomycin (OL) [22] could provide a model to unveil the mechanisms involved in the acquisition of the malignant phenotype. In the present investigation we have addressed the mechanisms and signaling pathways that control the down-regulation of β-F1-ATPase in colon cancer cells treated with OL with the purpose of advancing in the knowledge of the phenotype that is competent for tumor promotion [22]. The results have uncovered that glycolysis and oxidative phosphorylation are regulated by different mechanisms of gene expression. Moreover, the results highlight the relevance of translational control mediated by the activation of the stress kinases AMPK [23] and GCN2 [24, 25] to specifically repress the translation of β-mRNA and the promotion of the abnormal bioenergetics of mitochondria in the cancer cell. Overall, we stress that the activation of AMPK and GCN2-ATF4 marks the onset of colon cancer progression.

EXPERIMENTAL

Cellular treatments and siRNA silencing. Human colorectal carcionoma HCT116 cells were grown at 37ºC and 7% CO_2 in McCOY's 5A media supplemented with 10% fetal bovine serum. Cells were left untreated (M-type cells) or treated with 6 μM OL for 48h (G-type cells) [22]. Where indicated the cells were incubated with 0.1 mM AICAR for 48h. Transfections of AMPK plasmids [26] were carried out with Lipofectamine and Plus Reagent (Invitrogen). A plasmid encoding a mitochondrial version of green fluorescent protein was co-transfected with the plasmids of interest at a 1:10 ratio to assess transfeccion efficiencies. siRNA Quiagen s1702 used to suppress the expression of ATF4 was transfected using siPORT NeoFx reagent (Ambion/Applied Biosystems). An inefficient siRNA sequence, Silencer Select Negative Control number 1 plasmid (Ambion/Applied Biosystems), was used as a negative control and the siRNA of GAPDH was used as a positive control. The medium was changed at 24 h post-transfection and the cells were analyzed at 48h post-transfection for ATF4 expression.

Western blots. Cellular pellets were resuspended in lysis buffer containing 25mM Hepes, 2.5 mM EDTA, 1% Triton X-100, 1 mM PMSF and 5 μg/ml leupeptin. Extracts were centrifuged at 11,000g for 15 min at 4ºC. Protein concentration in the supernatants was determined with the Bradford reagent. Cellular proteins (7-20 μg) were fractionated on SDS-9% or SDS-15% PAGE and then transferred onto PVDF membranes. The primary antibodies used were: anti-β-F1-ATPase(1:50,000) [10], anti-Hsp60 (Stressgen SPA-807, 1:2,000), anti-GAPDH (1:20,000) and anti-PK (1:1,000) from Abcam, anti-SDH (1:500), anti-PDH (1:500) and anti-COX IV (1:250) from Invitrogen, anti-COX I (1:150) and anti-α-F1-ATPase (1:1,000) from Molecular Probe, anti-α-tubulin (1:5,000) and anti-LC3 (1:5,000) from Sigma, anti-β-catenin (BD Biosciences, 1:500), anti-GRK2 (1:500), anti-p53 (1:200), anti-HIF-1α (1:150), anti-PGC1α (1:250), anti-p70S6K (1:1,000), anti-HuR (1:200), anti-eIF2α (1:1,000) and anti-ATF4 (1:500) from Santa Cruz Biotechnology, anti-Akt (1:1,000), anti-p-Akt (1:1,000), anti-AMPK (1:1,000), anti-p-AMPK (1:1,000), anti p38 MAPK (1:1,000), anti-mTOR (1:1,000), anti-p-mTOR (1: 1,000) anti-4EBP1 (1:1,000), anti-p-4EBP1 (1:1,000), anti-p-p70S6K (1:1,000), anti-p-eIF2α (1: 1,000) and anti-p-GCN2 (1:2,000), anti-p-raptor (1:1,000), anti-p-S6 (1:1,000), anti-p-ACC (1:1,000), anti-ULK1 Ser^{555} (1:1,000) and anti-ULK1 Ser^{758} (1:1,000) from Cell Signaling, anti-GCN2 (1:2,000) [27], anti-c-Myc (1:400) from Roche Applied Science and anti-p62 (1:1,000) from Enzo Life Sciences. Secondary goat anti-rabbit, rabbit anti-goat and rabbit anti-mouse antibodies (1:5,000) were used for detection using a chemiluminescence detection method (ECL, Invitrogen). Membranes were exposed to X-ray films. Quantification of the immunoreactive bands (arbitrary units) was

accomplished using a Kodak DC120 Zoom digital camera and the Kodak 1D Image Analysis Software for Windows.

Quantitative RT-PCR analysis. RNA samples were extracted from the cells using the RNAeasy mini kit (QIAGEN). Total RNA samples were quantified using a Nanodrop ND-1000 spectrophotometer. RNA integrity was assessed with an Agilent 2100 Bioanalyzer. Reverse transcription (RT) reactions were performed using 1μg of total RNA and the High Capacity Reverse Transcription Kit (Applied Biosystems) with random primers. Primers were designed with Probe Finder Software (Roche Applied Science). The primers used were: β-F1-ATPase-F: cagcagattttggcaggtg, β-F1-ATPase-R: cttcaatgggtcccaccata; Hsp60-F: tgctatggctggagattttgt, Hsp60-R: cagcagcatccaataaagca; GAPDH-F: agccacatcgctcagacac, GAPDH-R: gcccaatacgaccaaatcc; G3BP1-F: ctttggtgggtttgtcactg, G3BP1-R: tgctgtctttcttcaggttcc; LC3-F: cgcaccttcgaacaaagag, LC3-R: ctcacccttgtatcgttctattatca; 18S-F: gcaattattccccatgaacg, 18S-R: gggacttaatcaacgcaagc; ATF4-F: tctccagcgacaaggctaa, ATF4-R: caatctgtcccggagaagg. Real-time PCR was performed using Power Sybr Green PCR Master Mix (Applied Biosystems) and LightCycler ® 2.0 Real-Time PCR System (Roche Applied Science). The relative expression of the mRNAs was determined using the comparative ΔΔCt method with GAPDH, G3BP1 GTPase (activating protein (SH3 domain) binding protein 1) or 18S (18S rRNA) as controls.

Determination of mitochondrial DNA (mtDNA) copy number. Cellular DNA (nDNA+mtDNA) was extracted from the cells ($4x10^5$) using the High Pure PCR Template Preparation Kit from Roche. Quantification of mtDNA (mtDNA/nDNA) was performed by qPCR in the LightCycler ® 2.0 Real-Time PCR System (Roche Applied Science) using 5 ng of DNA, 0.5 μM of primers and the PCR reaction mixtures LightCycler® FastStart DNA MasterPLUS SYBR Green I (Roche Applied Science). The nuclear ATP5B and the mitochondrial 12S rRNA encoded genes were chosen to determine the ratio of mtDNA to nDNA. The primers used were: 12S-F: cccagggttggtcaatttc, 12S-R: ctttacgccggcttctattg; hβ-F: cagcagattttggcaggtg, hβ-R: cttcaatgggtcccaccata. The relative mtDNA copy number was calculated using the ΔΔCt method and the 12S/hβ ratio used to compare the samples.

Metabolic Labeling and Immuno-precipitation. For pulse experiments, cells (~10^5) were incubated 20 min in cysteine-methionine-free medium. Metabolic labeling was initiated by addition of an aliquot of culture medium supplemented with 0.65 mCi of [^{35}S]-methionine/ml. After 30-45 min the radioactive medium was removed and the cells washed three times with PBS (phosphatebuffered saline) containing 5mM methionine and cysteine. Cellular pellets were resuspended in RIPA buffer (0.5M NaCl, 2% Triton X-100, 0.1M Tris-HCl pH 8.0, 0.2% SDS, 1% Na-DOC) supplemented with protease inhibitor cocktail (Roche) and freeze-thawed three times. Protein concentration was determined with the Bradford reagent. The radioactivity incorporated into TCA precipitable protein was determined [15]. Immunoprecipitations were carried out from 100 μg protein of cellular extracts using G-sepharose pre-coated with 6-7.5 μg of the IgGs of the following monoclonal antibodies: anti-Hsp60 (clone 17/9-15 G1), anti-β-F1-ATPase (clone 11/21-7 A8), anti-PK (clone 1415-21/24) or anti-GAPDH (clone 273A-E5) [28]. Pre-coating of G-sepharose was carried out overnight at 4ºC in 1 ml of RIPA buffer supplemented with 5 mg of BSA. After formation of the immune complexes, the resin was washed [21] and the immunoprecipitated material was resuspended in 1xSDS-PAGE sample buffer and loaded on a 9 % SDS-PAGE gel. Gels were further processed for fluorography and exposed to X-ray films.

Determination of adenine nucleotides. Approximately, 10^7 cells were scraped off from the plates in PBS. Cells were precipitated and extracted with 500 μl of a 6% perchloric acid solution. After centrifugation at 15,000g to remove cell debris, the resulting supernatants

were neutralized with 2% KOH and freeze-dried. Determination of the cellular content of ATP, ADP and AMP was carried out by standard enzymatic procedures.

Immunofluorescence microscopy. Cells were fixed with 4% paraformaldehyde for 20 minutes and processed for immunofluorescence. The primary antibody used was rabbit anti-LC3 antibody from Sigma (1:100). After three PBS rinses, the cells were incubated for 1h in the dark with anti-rabbit IgGs conjugated to Alexa-594 (1:1000). Cellular fluorescence was analyzed by confocal microscopy using a 63x1.4 oil plan-apocromate objective.

Glycolysis and cellular respiration. Lactate concentrations in the culture media were enzymatically determined as an index of glycolysis [22]. Oxygen consumption rates were determined in a XF24 Extracellular Flux Analyzer (Seahorse Bioscience). Cells were seeded in the microplates, treated as indicated and incubated at 37ºC and 7% CO_2 for 48h. The final concentration and order of injected substances was 6 μM OL, 0.75 mM 2,4-dinitrophenol (DNP), 1μM rotenone, and 1 μM antimycin [13].

Statistical analysis. Statistical analyses were performed using a two-tailed Student's *t* test. The results shown are the means±SEM. The number of experiments is indicated. A $p < 0.05$ was considered statistically significant.

RESULTS

Oligomycin treatment represses the bioenergetic phenotype of mitochondria. Comparative transcriptomic analysis of HCT116 cells treated (G) or non-treated (M) with OL (oligomycin) suggested a global repression of the metabolic and bioenergetic function of mitochondria in G-cells [22]. The results in Fig. 1a indicate that G-cells have a diminished complement of pyruvate dehydrogenase (PDH-E1α), succinate dehydrogenase (SDH-A), subunits I (mtDNA encoded) and IV (nDNA encoded) of cytochrome c oxidase and of subunits α and β of the H^+-ATP synthase when compared to non-treated M-cells. These changes occurred in the absence of relevant changes in the cellular content of the structural mitochondrial protein Hsp60 (heatshock protein 60) and in the abundance of the glycolytic markers GAPDH (glyceraldehyde-3-phosphate dehydrogenase) and PK (pyruvate kinase) (Fig. 1a). Therefore, both the mitochondrion (β-F1/Hsp60 ratio) and overall mitochondrial potential of OL-treated cells as assessed by its bioenergetic signature (β-F1/GAPDH ratio) [4], were significantly diminished when compared to controls (Fig. 1b). Interestingly, these changes also occurred in the absence of relevant changes in mtDNA copy number (Fig. 1b). Consistent with the enzymatic phenotype displayed, G-cells had lower activity of oxidative phosphorylation (OSR in Fig. 1c) and an increased flux of lactate production (Fig. 1d).

Inhibition of protein synthesis hampers the bioenergetic differentiation of mitochondria. Quantification by RT-qPCR of the cellular content of the mRNAs encoding β-F1-ATPase and GAPDH illustrated the lack of relevant differences in the abundance of these transcripts between M and G-cells (Fig. 2a). A slight but significant 15% reduction in Hsp60 mRNA levels was observed in G-cells (Fig. 2a) although this difference had no impact on protein expression (Fig. 1a). These findings indicate that down-regulation of β-F1-ATPase in G-cells (Fig. 1a) could not be ascribed to a limited activity of the transcription of the ATP5B gene or to a regulatory event affecting the abundance of its mRNA. Rather, the results suggest that β-F1-ATPase expression is being controlled at the level of mRNA translation.

To confirm this idea, we studied the initial rates of protein synthesis after a short time-pulse of ^{35}S-methionine in M- and G-cells. We observed no significant differences in the overall rate of protein synthesis between M- and G-cells (Fig. 2b). However, the results showed a significant 2-3 fold reduction in the relative rate of synthesis of β-F1-ATPase and

Hsp60, the two nuclear encoded mitochondrial proteins, in G-cells (Fig. 2b). In contrast, the relative rates of synthesis of the two glycolytic proteins were no different when compared to M-cells (Fig. 2b). These findings indicate that the switch from the M- to the G-phenotype of colon cancer HCT116 cells [22] involves the specific repression of the translation of the mRNAs encoding mitochondrial proteins. In this regard, reanalysis of the transcriptomic study carried out to compare M and G cells [22] further indicated a highly significant (Benjamini P value=5,4E-5) repression of the expression of a large number of the mitochondrial aminoacyl-tRNA synthetases in G-cells. The lack of changes observed in Hsp60 expression in G cells (Fig. 1a) despite a significant reduction in its initial rate of synthesis (Fig. 2b) further suggests the participation of mechanisms operating at the level of protein turnover.

Cellular adaptive response to OL treatment. Next, we monitored some of the relevant signaling pathways that are involved in the control of cell proliferation, survival and invasion and that might participate in the repression of the bioenergetic function of mitochondria. Interestingly, we found that HIF1α (hypoxia inducible factor 1 α) was not differentially expressed in G-cells when compared to M-cells (Fig. 3), consistent with the observation that OL blocks HIF1α expression [29]. Similar results were obtained for β-catenin, GRK2 (G protein-coupled receptor kinase 2), p38 MAPK (p38 mitogen-activated protein kinases) and both for the total and phosphorylated forms of the serine/threonine kinase Akt (v-akt murine thymoma viral oncogene) (Fig. 3). Notably, we found significant differences in the expression of the stress kinases AMPK and GCN2 supporting the activation of these pathways in cells with the G-phenotype (Fig. 3). Indeed, both the total and phosphorylated forms of AMPK were augmented in G- when compared to M-cells (Fig. 3). Consistent with the activation of AMPK we observed an increased cellular AMP/ATP ratio after short-term (2h) treatment of HCT116 cells with OL. Interestingly, the AMP/ATP ratio was not significantly different between M and G cells after 48h of treatment (Fig. 3). In the case of the GCN2 kinase, only the phosphorylated active form of the protein was augmented in cells with the G-phenotype (Fig. 3).

Downstream targets of AMPK and GCN2. AMPK is a master protein kinase that regulates cell metabolism [23] and controls the activity of essential mediators of the cellular adaptive response such as p53 (tumor protein p53), HuR (ELAV-like protein) and the mammalian target of rapamycin (mTOR). Consistent with the activation of AMPK in G-cells we observed a large phosphorylation of raptor (Fig. 4) together with the down-regulation of the cellular content of mTOR and HuR in the absence of relevant changes in p53 when compared to M-cells (Fig. 4). Interestingly, acetyl-CoA carboxylase (ACC), a well established target of AMPK that is phosphorylated and inhibited upon AMPK activation was not affected in G-cells (Fig. 4), indicating the relevance that the synthesis of lipids has as pathway to allow cellular proliferation in colon cancer cells. The serine/threonine kinase mTOR controls translation and autophagy [30]. In agreement with the lesser signaling through mTOR we observe an increase in the total cellular content of the cap-dependent translation repressor 4EBP1 (eukaryotic translation initiation factor 4E binding protein 1) [31] in G-cells (Fig. 4). The content of the phosphorylated form of 4EBP1 was also diminished in G-cells (Fig. 4) further supporting the sequestration of the rate limiting translation initiation factor 4E [32]. On the other hand, and to our surprise other downstream targets of mTOR such as p70S6K (ribosomal protein S6 kinase 70kDa polypeptide 1), its phosphorylated form (p-p70S6K) and that of its target the ribosomal protein S6 (p-S6) and of the transcription coactivator PGC1α (peroxisome proliferator-activated receptor gamma coactivator 1 α) revealed no-significant changes between both cellular phenotypes (Fig. 4). Likewise, and consistent with the

activation of GCN2 in G-cells (Fig. 3), we observed a significant increase in the cellular content of the transcription factor ATF4 when compared to M-cells (Fig. 4). It is well established that GCN2 represses translation via phosphorylation of eIF2α (eukaryotic translation initiation factor 2 α) and the subsequent up-regulation of the translation of ATF4. However, in our study both the content of eIF2α and of its phosphorylated form was significantly down-regulated (Fig. 4), what might suggest feedback inhibition of the phosphorylation of eIF2α after long-term (48 h) activation of GCN2. Overall, these results strongly suggest that a major point of regulation for promoting the repression of the bioenergetic function of mitochondria in G-cells is exerted at the level of translation by activation of the AMPK and GCN2 stress kinases.

Autophagy is enhanced in G-cells. The phosphorylation of raptor (Fig. 4) and of Ser-555 of the autophagy initiator kinase unc-51-like kinase 1 (ULK1) (Fig. 5a) suggested the AMPK-mediated inhibition of the mTOR signaling pathway and the subsequent activation of autophagy in cells with the G-phenotype [30]. Consistent with the mTOR-mediated activation of autophagy we also noted the dephosphorylation of Ser-758 of ULK1 in G-cells (Fig. 5a). Interestingly, a significant decrease in the cellular content of the p62 marker of autophagy was noted in G-cells (Fig. 5a). Gene expression analysis using the Affimetrix Platform also indicated the transcriptional activation of the autophagic LC3 (microtubule-associated protein 1 light chain 3 α) gene (fold change increase of 1.7 in G-cells, $p<0.009$, [22]). Quantification of the expression of LC3 mRNA by RT-qPCR showed a significant increase in its cellular content in G-cells when compared to M-cells (Fig. 5b). Moreover, western blot data confirmed that the ratio of the conjugated form of LC3II to LC3I, which is a marker of autophagosome formation, is significantly increased in the G-phenotype (Fig. 5b). The higher abundance of autophagosomes in G-cells was further confirmed by immunofluorescence microscopy (Fig. 5c). Overall, these findings support that the activation of autophagy is an additional pro-survival strategy of the cancer cell to mediate the phenotypic changes that accompany the acquisition of the tumor promoting behavior in response to a bioenergetic stressor.

AMPK activation and ATF4 mediate the inhibition of mitochondrial ATP synthesis. To assess the effect of the activation of the AMPK pathway in cellular bioenergetics we first determined the oxygen consumption rates of HCT116 cells (Fig. 6a). The results show a representative experiment of cellular O_2 consumption after the sequential addition of OL, DNP (2,4-dinitrophenol), rotenone and antimycin to the cells, illustrating a normal respiratory response to the inhibition of oxidative phosphorylation (OL), mitochondrial uncoupling (DNP) and the inhibition of respiration in HCT116 cells. Moreover, data in Fig. 6b indicate the linear response of the maximum (MRR), basal (BRR) and oligomycin sensitive (OSR) respiratory rate of the cells at increasing numbers. The activation of AMPK pathway by treating the cells with 5-aminoimidazole-4-carboxamide-1-β-4-ribofuranoside (AICAR), an analog of AMP that is widely used as an activator of the pathway, promoted a significant decrease in OSR in HCT116 cells concurrently with the phosphorylation of AMPK (Fig. 6c). AICAR was used at a concentration of 0.1 mM because titration experiments of its effect on the proliferation of HCT116 cells indicated a high toxicity of the compound above this concentration (data not shown). Moreover, the expression of a constitutively active AMPK mutant (α1CA, T172D), which is a truncated version that is not dependent on regulatory subunits to activate the pathway [26] as revealed by the phosphorylation of AMPK (Fig. 6d) also promoted a large inhibition of oligomycin sensitive respiration when compared to their respective controls (Fig. 6d). These findings indicate that activation of AMPK partially hinders the activity of the mitochondrial ATP synthase. Interestingly, and consistent with our

previous observation of the lack of changes in p-ACC in G- when compared to M-cells (Fig. 4), we show that the overexpression of α1CA (Fig. 6d) or AICAR treatment (Fig. 6c) does not affect the phosphorylation of ACC, stressing the relevance of lipogenesis for proliferation of HCT116 colon cancer cells.

To confirm that activation of AMPK participates in controlling mitochondrial oxidative phosphorylation in colon cancer cells we next studied the effect of AICAR on the rates of β-F1-ATPase synthesis (Fig. 7). The results demonstrated that the activation of AMPK significantly reduced the initial rate of β-F1-ATPase synthesis in the absence of relevant changes on overall protein synthesis and on the synthesis of Hsp60, GAPDH and PK (Fig. 7), indicating that the activation of AMPK participates in the repression of the bioenergetic function of colon cancer mitochondria.

To support the participation of the GCN2-ATF4 pathway in silencing the bioenergetic activity of mitochondria we determine the effect of silencing ATF4 in cellular respiration of M-cells (Fig. 8). The results obtained indicated that 40-60% silencing of ATF4 at both the mRNA and protein levels (Fig. 8a, b) resulted in a significant increase in oxidative phosphorylation (Fig. 8c) also supporting the participation of this pathway in promoting the repression of the bioenergetic activity of mitochondria in colon cancer.

DISCUSSION

We have recently documented that colon cancer progression requires the selection of cancer cells with a highly glycolytic phenotype due to the repression of the bioenergetic function of mitochondria [22]. However, the mechanisms and signaling pathways that trigger the down-regulation of β-F1-ATPase and hence of mitochondrial oxidative phosphorylation in colon cancer remained to be investigated. Colon cancer cells treated with oligomycin provide a model to decipher the mechanisms and signalling pathways that mediate the acquisition of the metabolic phenotype compatible with tumor progression [22, 33].

The results in this work illustrate that metabolic stress triggered by OL-treatment to the cells promotes the persistent activation of the stress-kinases AMPK and GCN2 (Fig. 9). AMPK is a S/T kinase that regulates energetic metabolism and is activated under conditions that elevate the AMP/ATP ratio, such as glucose deprivation, hypoxia and muscle contraction [34]. AMPK activation triggers important changes in downstream targeted proteins with a wide functional relevance in homeostatic adaptation of the cell including the regulation of mitochondrial biogenesis [35] and function [36], autophagy [30] and angiogenesis [37]. Consistent with the activation of AMPK in G-cells we report the phosphorylation of raptor, a significant inhibition of mTOR, the subsequent inhibition of the synthesis of mitochondrial proteins and the activation of autophagy (Fig. 9). The up-regulation of the expression of genes involved in angiogenesis and vascular development has already been described in G-cells [22]. GCN2 is also a stress kinase activated by nutrient deprivation and viral infection [24, 25] that represses the translation of most mRNAs but selectively increases translation of ATF4 [38]. Consistent with the activation of GCN2, we show that the content of ATF4 transcription factor is significantly increased in G-cells (Fig. 9). It is likely that the coordinated activation of AMPK and GCN2 mediate the repression of the translation of nuclear-encoded mRNAs of mitochondria via 4EBP1 and eIF2α, respectively (Fig. 9). These changes trigger a profound switch in cellular energetic metabolism to an enhanced glycolysis due to a diminished activity of oxidative phosphorylation (Fig. 9). Remarkably, we report that whereas the synthesis and expression of nuclear-encoded mitochondrial proteins is stringently dependent on the activity of cap-dependent translation, that of the enzymes of glycolysis is

not affected by interference with this pathway suggesting the existence of a specific pathway for translation of the mRNAs involved in glycolysis. Due to the essential cellular function of glycolysis, it is possible that translation of glycolytic mRNAs shares signaling pathways and mechanisms with translation of the mRNAs involved in cellular adaptation to stressful condition [27]. These findings provide the first indication that the mechanisms that control the expression of the enzymes of the two main pathways of energy metabolism (OXPHOS and glycolysis) are exerted independently and at a different level of regulation of gene expression. In addition, it is likely that metabolic adaptation also involves the participation of additional mechanisms acting at the level of protein turnover. The repression of the bioenergetic function of mitochondria, which is a reversible phenotypic trait of the cancer cell [22], is thus orchestred by the activation of the stress sensors AMPK and GCN2. In agreement with our findings (Fig. 9), it has been recently described the activation of AMPK in colorectal [39] and ovarian [40] carcinomas and the requirement of the GCN2-ATF4 pathway for maintaining metabolic homeostasis and tumor cell survival [38].

Interestingly, the repression of β-F1-ATPase expression observed in G-cells is not paralleled by changes in the cellular abundance of its mRNA. In fact, reduced β-F1-ATPase expression results from a translation masking event of β-mRNA in agreement with similar findings observed in human [19] and rat [18] carcinomas. It is tempting to suggest that the diminished expression of other mitochondrial proteins observed in G-cells (Fig. 1) could result by regulation of a common and presently unknown factor needed for translation of this particular set of nuclear-encoded mRNAs of mitochondria. Translation masking of β-mRNA during development [14] and in carcinogenesis [18, 21, 41] is due to the binding of specific RNABPs to the transcript. It has been suggested that regulated interactions within the ribonucleoprotein complex [42] hamper the efficient translation of β-mRNA [4]. Moreover, protein binding to β-mRNA was shown to depend on a low energy and oxidized state of the cell [43]. Consistent with these findings, it is possible that the increase in the AMP/ATP ratio observed at short term after treatment of the cells with OL could mediate the rapid silencing of β-mRNA by favoring the binding of repressor proteins onto the transcript (Fig. 9). In fact, AMPK activity has been correlated with the activity of some RNABPs such as HuR [44], a relevant RNABP involved in post-transcriptional regulation of gene expression that interacts with the 3'UTR of β-mRNA [41]. In agreement with recent findings [33], we observed that the activation of glycolysis in response to OL treatment provides enough ATP to recover a normal AMP/ATP ratio at long-term. Hence, it is likely that the persistent activation of AMPK observed in G-cells after 48h of OL-treatment is being mediated by additional regulators of the bioenergetically stressed cell.

AMPK activation is related to an increased mitochondrial biogenesis in muscle and endothelial cells via transcriptional regulation mediated by PGC1α/NRF/Tfam pathway [3, 35]. However, we do not observe changes in the expression of PGC1α in colon cancer stressed cells. In fact, our results indicate that the persistent activation of AMPK in stressed cells results in the repression of the bioenergetic differentiation of mitochondria by mechanisms controlled at the level of translation. This repression is most likely mediated via 4EBP1 for transcripts encoded in nuclear genes and by a lower expression of the mitochondrial aminoacyl-tRNA synthetases for the transcripts encoded in mtDNA. A general belief is that the activation of AMPK and the inhibition of mTOR are cytotoxic to cancer cells [32, 45]. However, we observed that persistent activation of AMPK and the inhibition of mTOR are required to establish the tumor-promoting phenotype of colon cancer cells by repression of the bioenergetic function of mitochondria [22]. In this regard, and consistent with our observations, it has been described that the inhibition of the mTOR pathway down-

regulates mitochondrial oxygen consumption and the ATP synthetic capacity [36]. In agreement with this, we show that AICAR treatment or the over-expression of a constitutively active mutant of AMPK, resulted in diminished ATP synthetic capacity and the inhibition of β-F1-ATPase synthesis. These findings strongly support that the activity of the mTOR pathway is essential for maintaining the bioenergetic function of mitochondria [36] and specifically of the synthesis of β-F1-ATPase. Within this frame, and in contrast to the beneficial effects of targeting mTOR in cancer [32, 45, 46], our results raise a reasonable argument against therapies targeting the activation of AMPK and the inhibition of mTOR for the treatment of colon cancer. In agreement with our observation, it has been described that the inhibition of AMPK sensitizes cancer cells to chemotherapy [47]. It is likely that these differences in cell response might stem from cell-type specific changes in the mechanisms that regulate the biogenesis and function of mitochondria [3].

AMPK and GCN2 are activated by stress signaling such as glucose deprivation, hypoxia, starvation of amino acids, etc [24, 25, 34]. Interestingly, none of these stimuli, including hypoxia, seem to operate in our model. However, it is remarkable that the energetic stress that activated AMPK in G-cells is very similar from the mechanistic point of view to the HIF–independent hypoxia-induced energy stress that activates mechanisms of energy conservation to promote survival under stressful conditions [48]. In this regard, we suggest that a product of mitochondrial metabolism such as reactive oxygen species (ROS) could act as signaling metabolite to maintain the cellular stress and the persistent activation of AMPK [49] and GCN2. The scenario where small molecules define the cellular energy status offer very attractive hypothesis to explain the mitochondrial phenotype and its short-term adaptive response upon changes in the metabolic condition of the cell. In this regard, we show that in response to energy stress the autophagic pathway is activated in G-cells perhaps as a strategy to eliminate the damaged proteins produced during adaptation to stress in order to optimize the limited energy supplies [30]. We show that the activation of the GCN2/eIF2α/ATF4 pathway is involved in minimizing the bioenergetic function of mitochondria, allowing cells to conserve resources and the reconfiguration of gene expression to manage the energetic stress imposed, leading to the activation of glycolysis as alternative energy provision pathway (Fig. 9). In this regard, our results provide the first demonstration illustrating the implication of this pathway to control the stress-response when the mitochondrial bioenergetic function is impeded. Consistent with this, we show that the silencing of ATF4 restores the bioenergetic function of mitochondria.

Overall, we conclude that persistent activation of AMPK and GCN2 regulate the balance between glycolysis and aerobic metabolism specifically repressing the translation of nuclear-encoded mitochondrial proteins. Activation of these signaling pathways is essential to implement a successful response that could allow cancer cells to survive under metabolic stress. Finally, our results open new insights in the pathways involved in the acquisition of a tumor promoter phenotype that implies a deregulated mitochondrial function, highlighting the importance that the organelle has as a tumor suppressor.

Acknowledgements. We are grateful to Drs. J.J. Berlanga, D. Carling, D. Carmena, C. De Haro and A. Woods for helpful discussion and suggestions and for providing different reagents. We also thank to F. Carrasco, M. Chamorro and C. Núñez de Arenas for their support in qPCRs and expert technical assistance. The authors declare no conflict of interest.

Author contributions: IMR and MSA carried out experiments. IMR, MSA and JMC contributed in the analysis of the data. IMR and JMC designed experiments and wrote the manuscript. All authors have read and approved the final version of the manuscript.

Funding. This work was supported by grants from Ministerio de Educación y Ciencia (BFU2010-18903), the Centro de Investigación Biomédica en Red de Enfermedades Raras (CIBERER) del ISCIII and Comunidad de Madrid (S2010/BMD-2402), Spain. The CBMSO receives an institutional grant from Fundación Ramón Areces. IMR is the recipient of a pre-doctoral fellowship from JAE-CSIC.

REFERENCES

1 Cuezva, J. M., Ortega, A. D., Willers, I., Sanchez-Cenizo, L., Aldea, M. and Sanchez-Arago, M. (2009) The tumor suppressor function of mitochondria: translation into the clinics. Biochim Biophys Acta. **1792**, 1145-1158

2 Wallace, D. C. (2005) A mitochondrial paradigm of metabolic and degenerative diseases, aging, and cancer: a dawn for evolutionary medicine. Annu Rev Genet. **39**, 359-407

3 Scarpulla, R. C. (2008) Transcriptional paradigms in mammalian mitochondrial biogenesis and function. Physiol Rev. **88**, 611-638

4 Willers, I. M. and Cuezva, J. M. (2011) Post-transcriptional regulation of the mitochondrial H(+)-ATP synthase: A key regulator of the metabolic phenotype in cancer. Biochim Biophys Acta. **1807**, 543-551

5 Boyer, P. D. (1997) The ATP synthase--a splendid molecular machine. Annu Rev Biochem. **66**, 717-749

6 Hanahan, D. and Weinberg, R. A. (2011) Hallmarks of cancer: the next generation. Cell. **144**, 646-674

7 Bissell, M. J. and Hines, W. C. (2011) Why don't we get more cancer? A proposed role of the microenvironment in restraining cancer progression. Nat Med. **17**, 320-329

8 DeBerardinis, R. J., Lum, J. J., Hatzivassiliou, G. and Thompson, C. B. (2008) The biology of cancer: metabolic reprogramming fuels cell growth and proliferation. Cell Metab. **7**, 11-20

9 Lopez-Rios, F., Sanchez-Arago, M., Garcia-Garcia, E., Ortega, A. D., Berrendero, J. R., Pozo-Rodriguez, F., Lopez-Encuentra, A., Ballestin, C. and Cuezva, J. M. (2007) Loss of the mitochondrial bioenergetic capacity underlies the glucose avidity of carcinomas. Cancer Res. **67**, 9013-9017

10 Cuezva, J. M., Krajewska, M., de Heredia, M. L., Krajewski, S., Santamaria, G., Kim, H., Zapata, J. M., Marusawa, H., Chamorro, M. and Reed, J. C. (2002) The bioenergetic signature of cancer: a marker of tumor progression. Cancer Res. **62**, 6674-6681

11 Shin, Y. K., Yoo, B. C., Chang, H. J., Jeon, E., Hong, S. H., Jung, M. S., Lim, S. J. and Park, J. G. (2005) Down-regulation of mitochondrial F1F0-ATP synthase in human colon cancer cells with induced 5-fluorouracil resistance. Cancer Res. **65**, 3162-3170

12 Sanchez-Arago, M., Cuezva JM. (2011) The bioenergetic signature of isogenic colon cancer cells predicts the cell death response to treatment with 3-bromopyruvate, iodoacetate or 5-fluorouracil. J Transl Med. **9(1)**, 19

13 Sanchez-Cenizo, L., Formentini, L., Aldea, M., Ortega, A. D., Garcia-Huerta, P., Sanchez-Arago, M. and Cuezva, J. M. (2010) Up-regulation of the ATPase inhibitory factor 1 (IF1) of the mitochondrial H+-ATP synthase in human tumors mediates the metabolic shift of cancer cells to a Warburg phenotype. J Biol Chem. **285**, 25308-25313

14 Izquierdo, J. M. and Cuezva, J. M. (1997) Control of the translational efficiency of beta-F1-ATPase mRNA depends on the regulation of a protein that binds the 3' untranslated region of the mRNA. Mol Cell Biol. **17**, 5255-5268

15 Izquierdo, J. M., Ricart, J., Ostronoff, L. K., Egea, G. and Cuezva, J. M. (1995) Changing patterns of transcriptional and post-transcriptional control of beta-F1-ATPase gene expression during mitochondrial biogenesis in liver. J Biol Chem. **270**, 10342-10350

16 Tvrdik, P., Kuzela, S. and Houstek, J. (1992) Low translational efficiency of the F1-ATPase beta-subunit mRNA largely accounts for the decreased ATPase content in brown adipose tissue mitochondria. FEBS Lett. **313**, 23-26
17 Martinez-Diez, M., Santamaria, G., Ortega, A. D. and Cuezva, J. M. (2006) Biogenesis and Dynamics of Mitochondria during the Cell Cycle: Significance of 3'UTRs. PLoS One. **1**, e107
18 de Heredia, M. L., Izquierdo, J. M. and Cuezva, J. M. (2000) A conserved mechanism for controlling the translation of beta-F1-ATPase mRNA between the fetal liver and cancer cells. J Biol Chem. **275**, 7430-7437
19 Willers, I. M., Isidoro, A., Ortega, A. D., Fernandez, P. L. and Cuezva, J. M. (2010) Selective inhibition of beta-F1-ATPase mRNA translation in human tumours. Biochem J. **426**, 319-326
20 Margeot, A., Blugeon, C., Sylvestre, J., Vialette, S., Jacq, C. and Corral-Debrinski, M. (2002) In Saccharomyces cerevisiae, ATP2 mRNA sorting to the vicinity of mitochondria is essential for respiratory function. Embo J. **21**, 6893-6904
21 Ortega, A. D., Willers, I. M., Sala, S. and Cuezva, J. M. (2010) Human G3BP1 interacts with beta-F1-ATPase mRNA and inhibits its translation. J Cell Sci. **123**, 2685-2696
22 Sanchez-Arago, M., Chamorro, M. and Cuezva, J. M. (2010) Selection of cancer cells with repressed mitochondria triggers colon cancer progression. Carcinogenesis. **31**, 567-576
23 Hardie, D. G., Scott, J. W., Pan, D. A. and Hudson, E. R. (2003) Management of cellular energy by the AMP-activated protein kinase system. FEBS Lett. **546**, 113-120
24 Berlanga, J. J., Santoyo, J. and De Haro, C. (1999) Characterization of a mammalian homolog of the GCN2 eukaryotic initiation factor 2alpha kinase. Eur J Biochem. **265**, 754-762
25 Berlanga, J. J., Ventoso, I., Harding, H. P., Deng, J., Ron, D., Sonenberg, N., Carrasco, L. and de Haro, C. (2006) Antiviral effect of the mammalian translation initiation factor 2alpha kinase GCN2 against RNA viruses. Embo J. **25**, 1730-1740
26 Fryer, L. G., Foufelle, F., Barnes, K., Baldwin, S. A., Woods, A. and Carling, D. (2002) Characterization of the role of the AMP-activated protein kinase in the stimulation of glucose transport in skeletal muscle cells. Biochem J. **363**, 167-174
27 Harding, H. P., Novoa, I., Zhang, Y., Zeng, H., Wek, R., Schapira, M. and Ron, D. (2000) Regulated translation initiation controls stress-induced gene expression in mammalian cells. Mol Cell. **6**, 1099-1108
28 Acebo, P., Giner, D., Calvo, P., Blanco-Rivero, A., Ortega, A. D., Fernandez, P. L., Roncador, G., Fernandez-Malave, E., Chamorro, M. and Cuezva, J. M. (2009) Cancer abolishes the tissue type-specific differences in the phenotype of energetic metabolism. Transl Oncol. **2**, 138-145
29 Gong, Y. and Agani, F. H. (2005) Oligomycin inhibits HIF-1alpha expression in hypoxic tumor cells. Am J Physiol Cell Physiol. **288**, C1023-1029
30 Sarbassov, D. D., Ali, S. M. and Sabatini, D. M. (2005) Growing roles for the mTOR pathway. Curr Opin Cell Biol. **17**, 596-603
31 Brunn, G. J., Hudson, C. C., Sekulic, A., Williams, J. M., Hosoi, H., Houghton, P. J., Lawrence, J. C., Jr. and Abraham, R. T. (1997) Phosphorylation of the translational repressor PHAS-I by the mammalian target of rapamycin. Science. **277**, 99-101

32 Silvera, D., Formenti, S. C. and Schneider, R. J. (2010) Translational control in cancer. Nat Rev Cancer. **10**, 254-266
33 Hao, W., Chang, C. P., Tsao, C. C. and Xu, J. (2010) Oligomycin-induced bioenergetic adaptation in cancer cells with heterogeneous bioenergetic organization. J Biol Chem. **285**, 12647-12654
34 Kahn, B. B., Alquier, T., Carling, D. and Hardie, D. G. (2005) AMP-activated protein kinase: ancient energy gauge provides clues to modern understanding of metabolism. Cell Metab. **1**, 15-25
35 Jeninga, E. H., Schoonjans, K. and Auwerx, J. (2010) Reversible acetylation of PGC-1: connecting energy sensors and effectors to guarantee metabolic flexibility. Oncogene. **29**, 4617-4624
36 Schieke, S. M., Phillips, D., McCoy, J. P., Jr., Aponte, A. M., Shen, R. F., Balaban, R. S. and Finkel, T. (2006) The mammalian target of rapamycin (mTOR) pathway regulates mitochondrial oxygen consumption and oxidative capacity. J Biol Chem. **281**, 27643-27652
37 Ouchi, N., Shibata, R. and Walsh, K. (2005) AMP-activated protein kinase signaling stimulates VEGF expression and angiogenesis in skeletal muscle. Circ Res. **96**, 838-846
38 Ye, J., Kumanova, M., Hart, L. S., Sloane, K., Zhang, H., De Panis, D. N., Bobrovnikova-Marjon, E., Diehl, J. A., Ron, D. and Koumenis, C. (2010) The GCN2-ATF4 pathway is critical for tumour cell survival and proliferation in response to nutrient deprivation. Embo J. **29**, 2082-2096
39 Baba, Y., Nosho, K., Shima, K., Meyerhardt, J. A., Chan, A. T., Engelman, J. A., Cantley, L. C., Loda, M., Giovannucci, E., Fuchs, C. S. and Ogino, S. (2010) Prognostic significance of AMP-activated protein kinase expression and modifying effect of MAPK3/1 in colorectal cancer. Br J Cancer. **103**, 1025-1033
40 Buckendahl, A. C., Budczies, J., Fiehn, O., Darb-Esfahani, S., Kind, T., Noske, A., Weichert, W., Sehouli, J., Braicu, E., Dietel, M. and Denkert, C. (2011) Prognostic impact of AMP-activated protein kinase expression in ovarian carcinoma: correlation of protein expression and GC/TOF-MS-based metabolomics. Oncol Rep. **25**, 1005-1012
41 Ortega, A. D., Sala, S., Espinosa, E., Gonzalez-Baron, M. and Cuezva, J. M. (2008) HuR and the bioenergetic signature of breast cancer: a low tumor expression of the RNA-binding protein predicts a higher risk of disease recurrence. Carcinogenesis. **29**, 2053-2061
42 Keene, J. D. (2007) RNA regulons: coordination of post-transcriptional events. Nat Rev Genet. **8**, 533-543
43 Izquierdo, J. M. and Cuezva, J. M. (2005) Epigenetic regulation of the binding activity of translation inhibitory proteins that bind the 3' untranslated region of beta-F1-ATPase mRNA by adenine nucleotides and the redox state. Arch Biochem Biophys. **433**, 481-486
44 Wang, W., Fan, J., Yang, X., Furer-Galban, S., Lopez de Silanes, I., von Kobbe, C., Guo, J., Georas, S. N., Foufelle, F., Hardie, D. G., Carling, D. and Gorospe, M. (2002) AMP-activated kinase regulates cytoplasmic HuR. Mol Cell Biol. **22**, 3425-3436
45 van Veelen, W., Korsse, S. E., van de Laar, L. and Peppelenbosch, M. P. (2011) The long and winding road to rational treatment of cancer associated with LKB1/AMPK/TSC/mTORC1 signaling. Oncogene. **30**, 2289-2303

46 Janes, M. R., Limon, J. J., So, L., Chen, J., Lim, R. J., Chavez, M. A., Vu, C., Lilly, M. B., Mallya, S., Ong, S. T., Konopleva, M., Martin, M. B., Ren, P., Liu, Y., Rommel, C. and Fruman, D. A. (2010) Effective and selective targeting of leukemia cells using a TORC1/2 kinase inhibitor. Nat Med. **16**, 205-213

47 Kim, H. S., Hwang, J. T., Yun, H., Chi, S. G., Lee, S. J., Kang, I., Yoon, K. S., Choe, W. J., Kim, S. S. and Ha, J. (2008) Inhibition of AMP-activated protein kinase sensitizes cancer cells to cisplatin-induced apoptosis via hyper-induction of p53. J Biol Chem. **283**, 3731-3742

48 Liu, L., Cash, T. P., Jones, R. G., Keith, B., Thompson, C. B. and Simon, M. C. (2006) Hypoxia-induced energy stress regulates mRNA translation and cell growth. Mol Cell. **21**, 521-531

49 Yun, H., Lee, M., Kim, S. S. and Ha, J. (2005) Glucose deprivation increases mRNA stability of vascular endothelial growth factor through activation of AMP-activated protein kinase in DU145 prostate carcinoma. J Biol Chem. **280**, 9963-9972

Figure legends

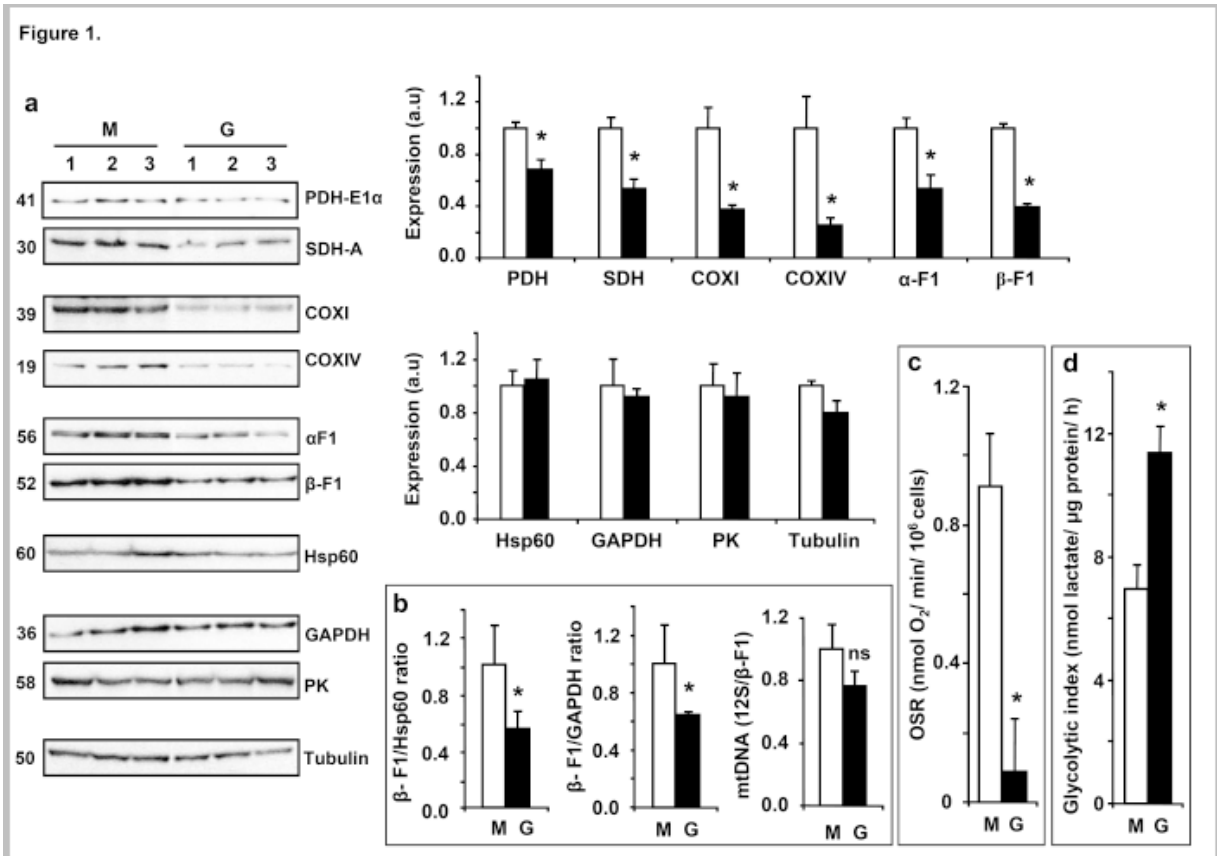

Figure 1. Oligomycin treatment represses the bioenergetic function of mitochondria. HCT116 cells were incubated with oligomycin (OL) (closed bars, G) or left untreated (open bars, M) to promote changes in the bioenergetic phenotype. **a,** Representative western blots of the expression of PDH-E1α, SDH-A, COXI, COXIV, α-F1-ATPase, β-F1-ATPase, Hsp60, GAPDH, PK and tubulin in three different preparations (lanes 1-3) of M and G cells are shown. **b,** The mitochondrial (β-F1-ATPase/ Hsp60) and cellular (β-F1-ATPase/ GAPDH) normalized expression of β-F1-ATPase and the relative mtDNA copy number (12S/β-F1 ratio) are indicated. In **a** and **b**, the histograms show the quantification of the bands normalized to the mean value in control M-cells. **c and d,** The rates of OL-sensitive respiration and of lactate production were determined, respectively. The results shown are the mean ±SEM of at least three determinations. * P< 0.05 when compared to M-cells by Student's *t*-test. The molecular mass of each protein is indicated on the left hand side of the blot.

Figure 2.

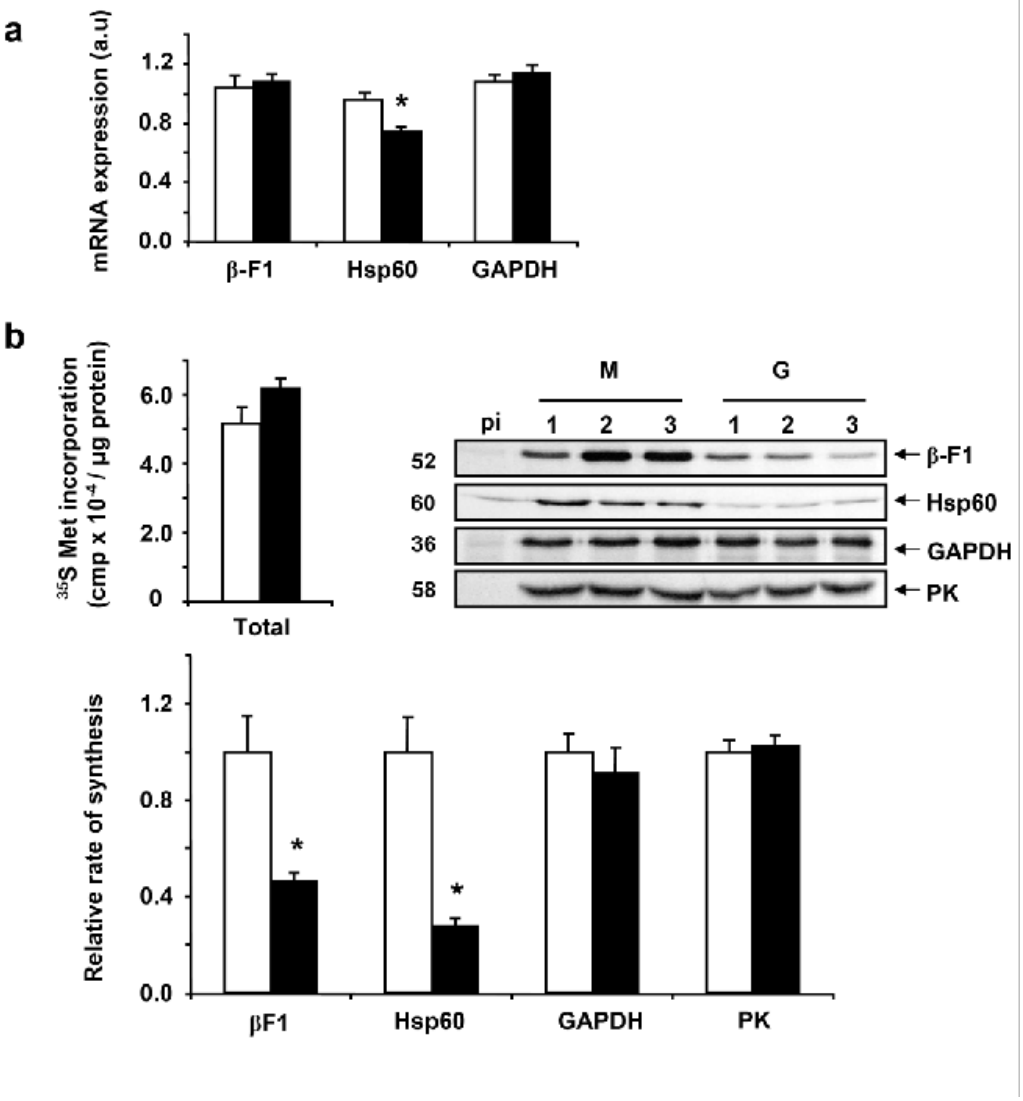

Figure 2. Translational control hampers the bioenergetic function of mitochondria. HCT116 cells were incubated with OL (closed bars, G) or left untreated (open bars, M). **a,** Cellular RNA was extracted and the relative mRNA abundance of β-F1-ATPase (β-F1), Hsp60 and GAPDH determined by qPCR. The results shown are the mean ±SEM of three experiments. **b,** Determination of the *in vivo* rate of β-F1, Hsp60, GAPDH and PK synthesis in M and G cells after metabolic labeling with ^{35}S-methionine followed by immunoprecipitation (^{35}S-IP). The radioactivity incorporated into TCA precipitable protein (Total) was determined. The histograms show the mean ±SEM of the quantification of the bands normalized to the mean value in control cells from three-six different preparations. p.i. non-specific immunoglobulin. * $P < 0.05$ when compared to M-cells by Student's *t*-test. The molecular mass of each protein is indicated on the left hand side of the blot.

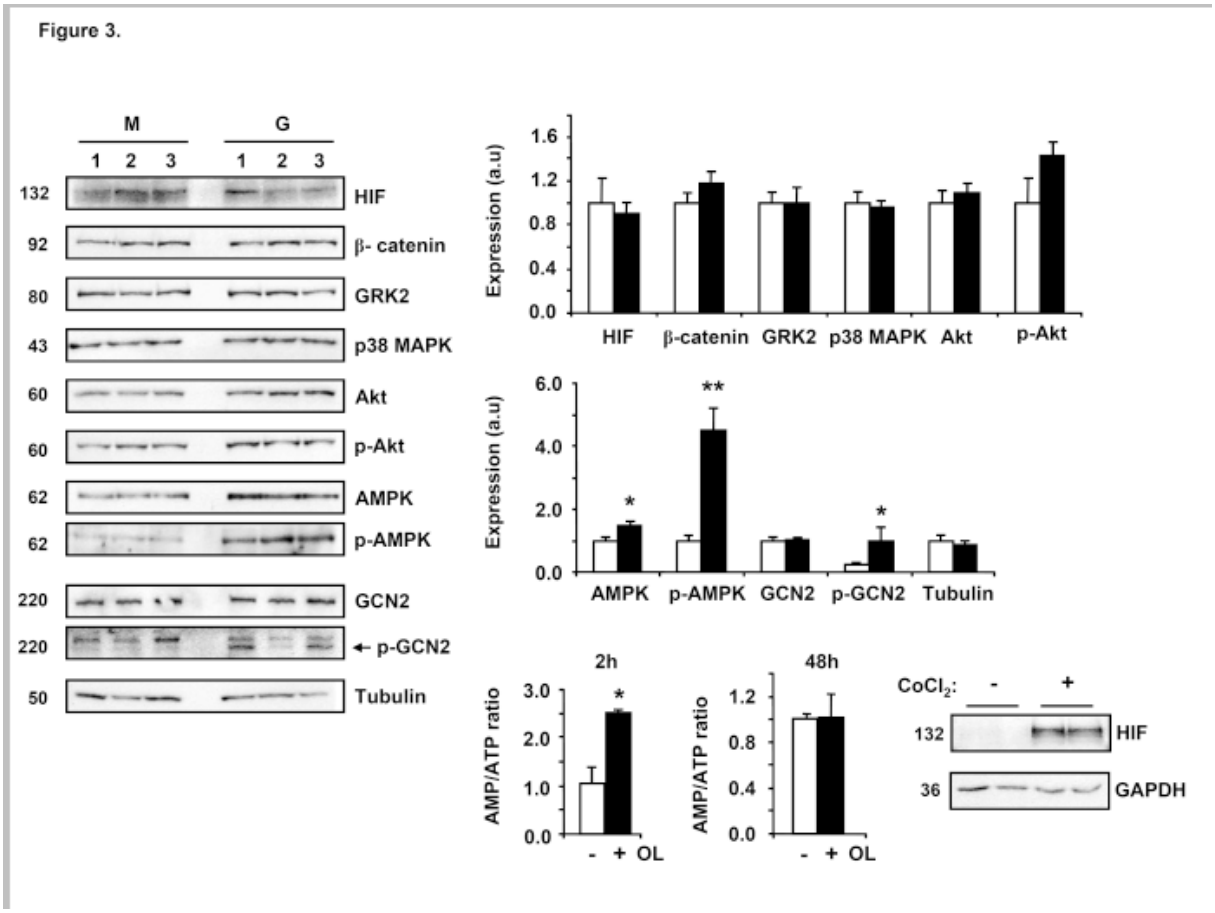

Figure 3. Cellular adaptive response to energetic stress involves the activation of AMPK and GCN2. HCT116 cells were incubated with OL (closed bars, G) or left untreated (open bars, M). Representative western blots of the expression of HIF1α, β-catenin, GRK2, p38 MAPK, Akt, p-Akt, AMPK, p-AMPK, GCN2, p-GCN2 and tubulin in three different preparations (lanes 1-3) of M and G cells are shown. The histograms show the quantification of the bands normalized to the mean value in control M-cells. The results shown are the mean ±SEM of at least three determinations. The AMP/ATP ratio was determined in M-cells after 2h or 48h treatment with OL and normalized to the mean value in untreated cells. The results shown are the mean ±SEM of nine determinations. HCT116 cells incubated with 200 μM $CoCl_2$ for 6h reveal the induction of HIF1α, a positive control to verify the specificity of the antibody used in the study. * $P< 0.05$ and ** $P<0.001$ when compared to M or untreated cells by Student's *t*-test. The molecular mass of each protein is indicated on the left hand side of the blot.

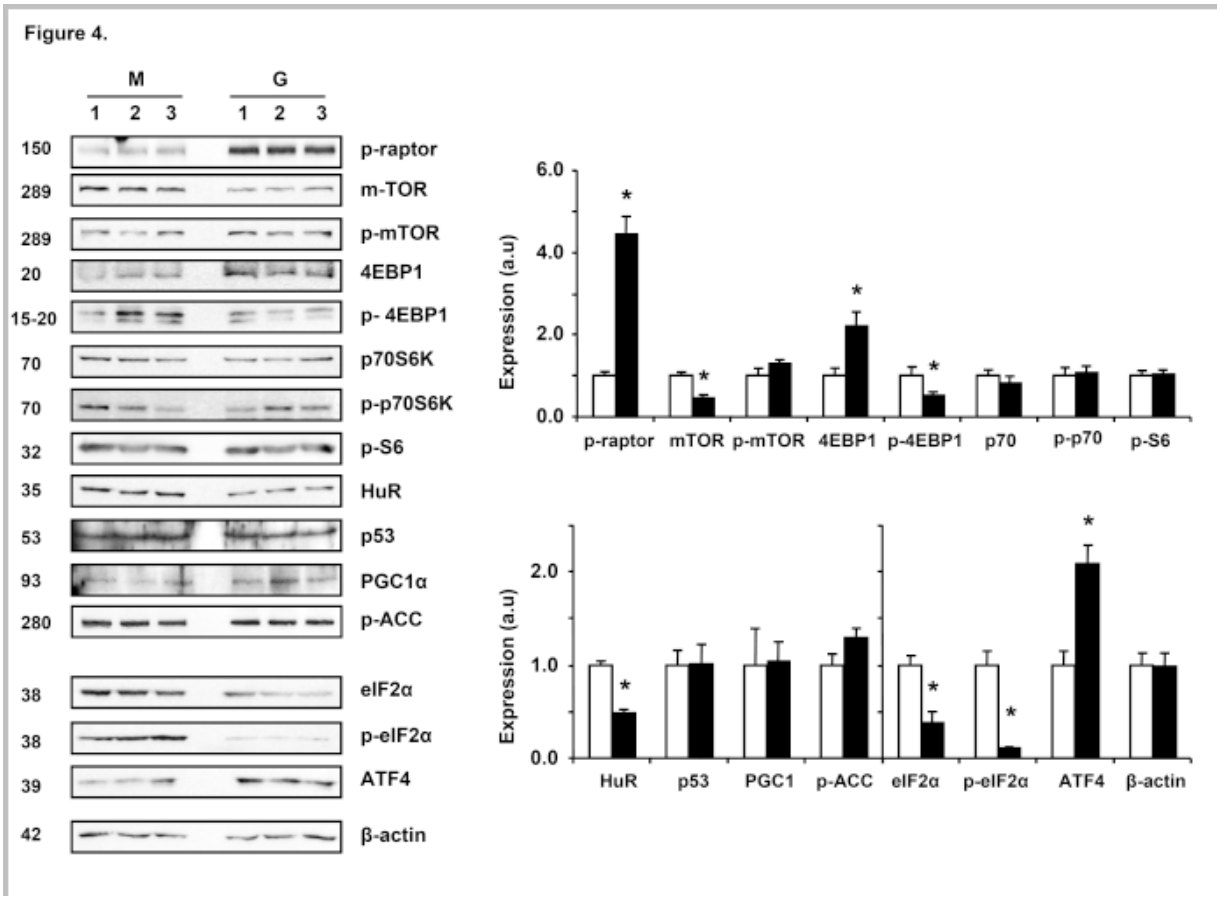

Figure 4. Energetic stress triggers significant changes in downstream targets of AMPK and GCN2. HCT116 cells were incubated with OL (closed bars, G) or left untreated (open bars, M). Representative western blots of the expression of p-raptor, mTOR, p-mTOR, 4EBP1, p-4EBP1, p70S6K, p-p70S6K, p-S6, HuR, p53, PGC1α, p-ACC, eIF2α, p-eIF2α, ATF4 and β-actin in three different preparations (lanes 1-3) of M and G cells are shown. The histograms show the quantification of the bands normalized to the mean value in control M-cells. The results shown are the mean ±SEM of three-nine determinations. * $P< 0.05$ and ** $P<0.001$ when compared to M cells by Student's *t*-test.

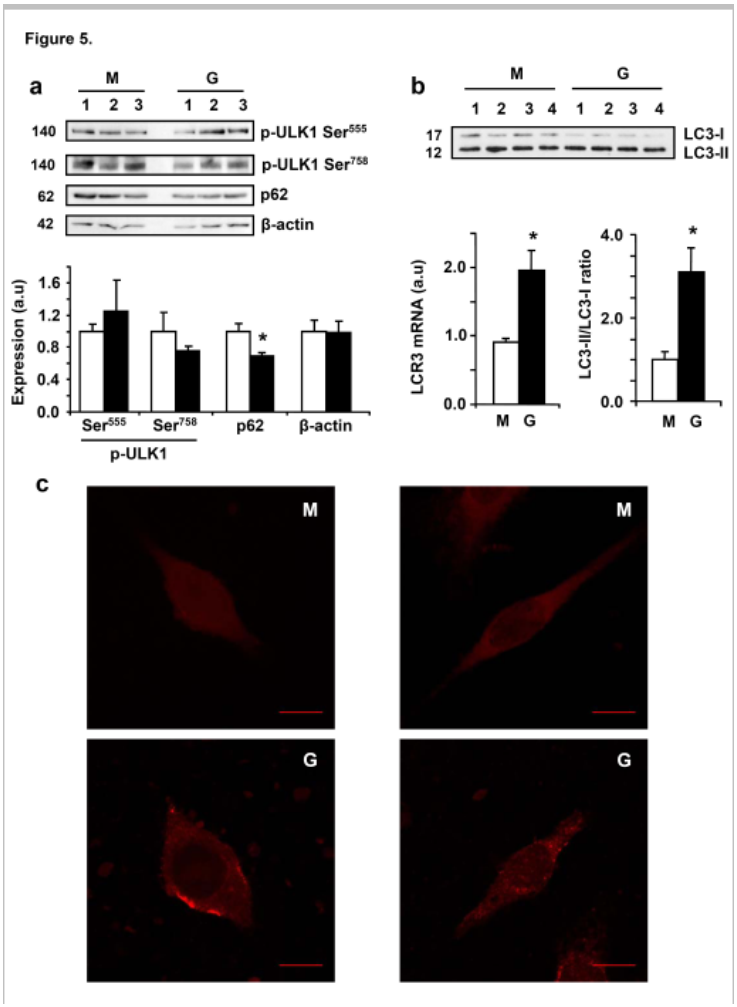

Figure 5. Inhibition of mTOR triggers the activation of autophagy. HCT116 cells were incubated with OL (closed bars, G) or left untreated (open bars, M). **a,** Representative western blots of the expression of p-ULK1 in Ser^{555}, p-ULK1 in Ser^{758} and p62 in three different preparations (lanes 1-3) of M and G cells are shown. The histograms show the quantification of the bands normalized to β-actin and to the mean value in control M-cells. The results shown are the mean ±SEM of three determinations. * $P< 0.05$ when compared to M cells by Student's *t*-test. **b,** Cellular mRNA was extracted and LC3 mRNA was determined by qPCR. The results shown are the mean ±SEM of three experiments. Analysis of LC3-I and its conjugated LC3-II form in four different preparations (lanes 1-4) of M and G cells by western blotting. The LC3-II/LC3-I ratio was normalized to the mean value in control M-cells is represented in the histogram. The results shown are the mean ±SEM of four determinations. * $P< 0.05$ when compared to M-cells by Student's *t*-test. **c,** Immunofluorescence microscopy of HCT116 cells incubated with OL for 48h (G, lower panels) or left untreated (M, upper panels), stained with anti-LC3 antibody. Images (x63) in G-cells illustrate the presence of autophagosomes (red cytoplasmic immunostaining). *Bar*, 10 μm. The molecular mass of each protein is indicated on the left hand side of the blot.

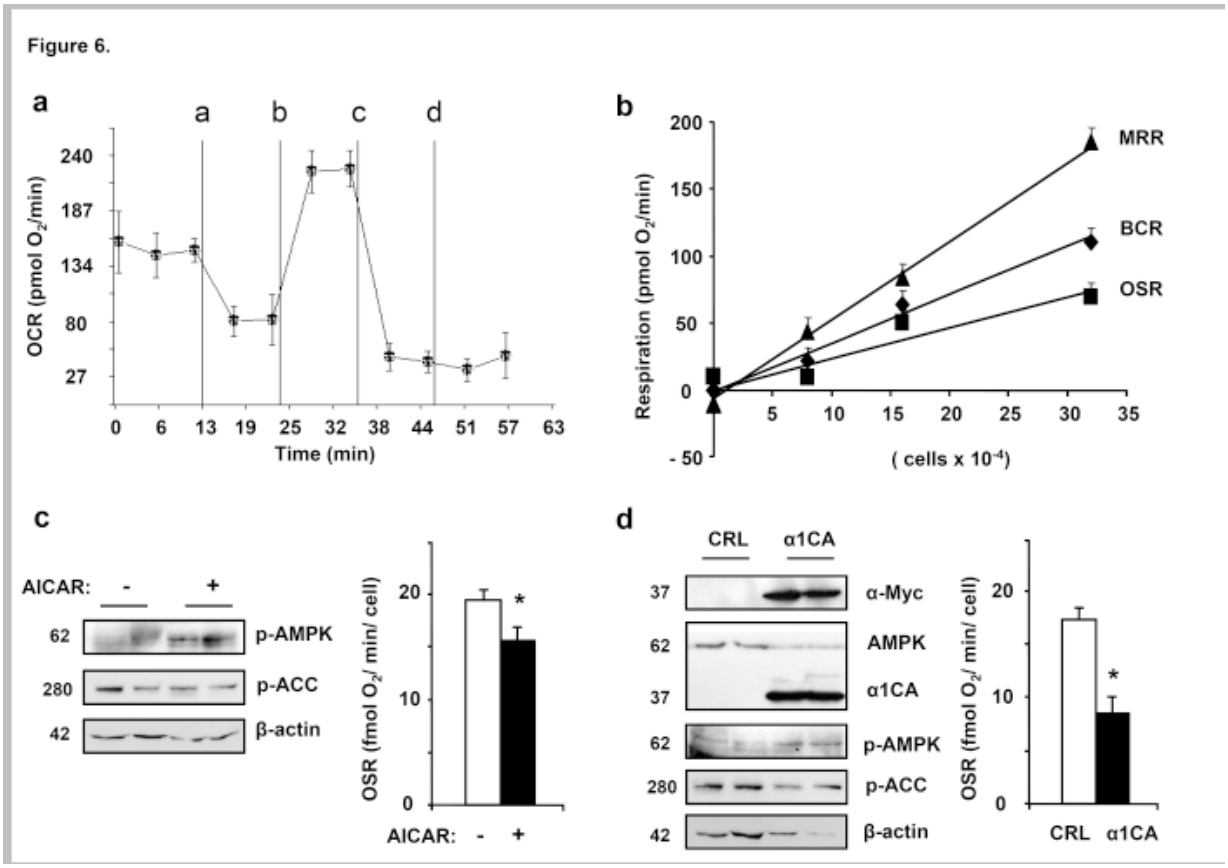

Figure 6. AMPK activation promotes the inhibition of oxidative phosphorylation. HCT116 cells were seeded at various densities in Seahorse plates. **a,** Illustrates the oxygen consumption rates after the sequential addition of OL (a), DNP (b), rotenone (c) and antimycin (d) to the cells. **b,** The plot show the linear response of the basal (BCR), OL-sensitive (OSR) and maximum (DNP-induced, MRR) respiratory rates at various cell densities. **c,** Incubation of M-cells with 0.1 mM AICAR promoted a significant decrease in OSR (closed bars) when compared with untreated (open bars) cells. The results shown are the mean ±SEM of three experiments. Representative western blots of the expression of p-AMPK and p-ACC are shown. **d,** Expression of a constitutively active AMPK mutant (α1CA), as revealed by western blot with either anti-Myc-tag or anti-AMPK, promotes a large inhibition of OSR (closed bars) when compared to control GFP transfected cells (open bars). The results shown are the mean ±SEM of three experiments. * P< 0.05 when compared to control cells by Student's *t*-test. Representative western blots of the expression of p-AMPK and p-ACC are shown. The molecular mass of each protein is indicated on the left hand side of the blot.

Figure 7.

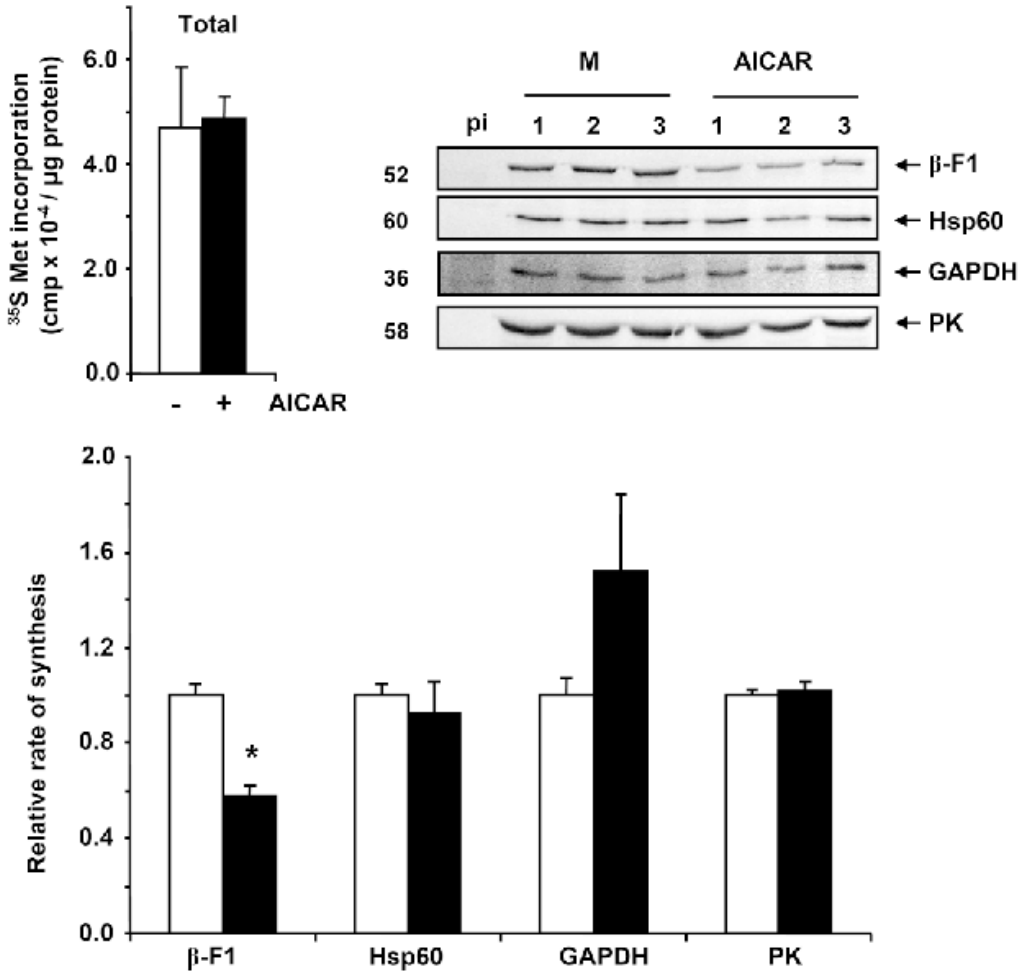

Figure 7. AMPK activation inhibits β-F1-ATPase synthesis. HCT116 cells were incubated with 0.1mM AICAR (closed bars) or left untreated (open bars). Determination of the in vivo rate of β-F1, Hsp60, GAPDH and PK synthesis in AICAR treated and untreated cells after metabolic labeling with ^{35}S-methionine followed by immunoprecipitation (^{35}S-IP). The radioactivity incorporated into TCA precipitable protein (Total) was determined. The histograms show the mean ±SEM of the quantification of the bands normalized to the mean value in control cells from three different preparations (lanes 1-3). p.i. non-specific immunoglobulin. * $P< 0.05$ when compared to untreated cells by Student's *t*-test. The molecular mass of each protein is indicated on the left hand side of the blot.

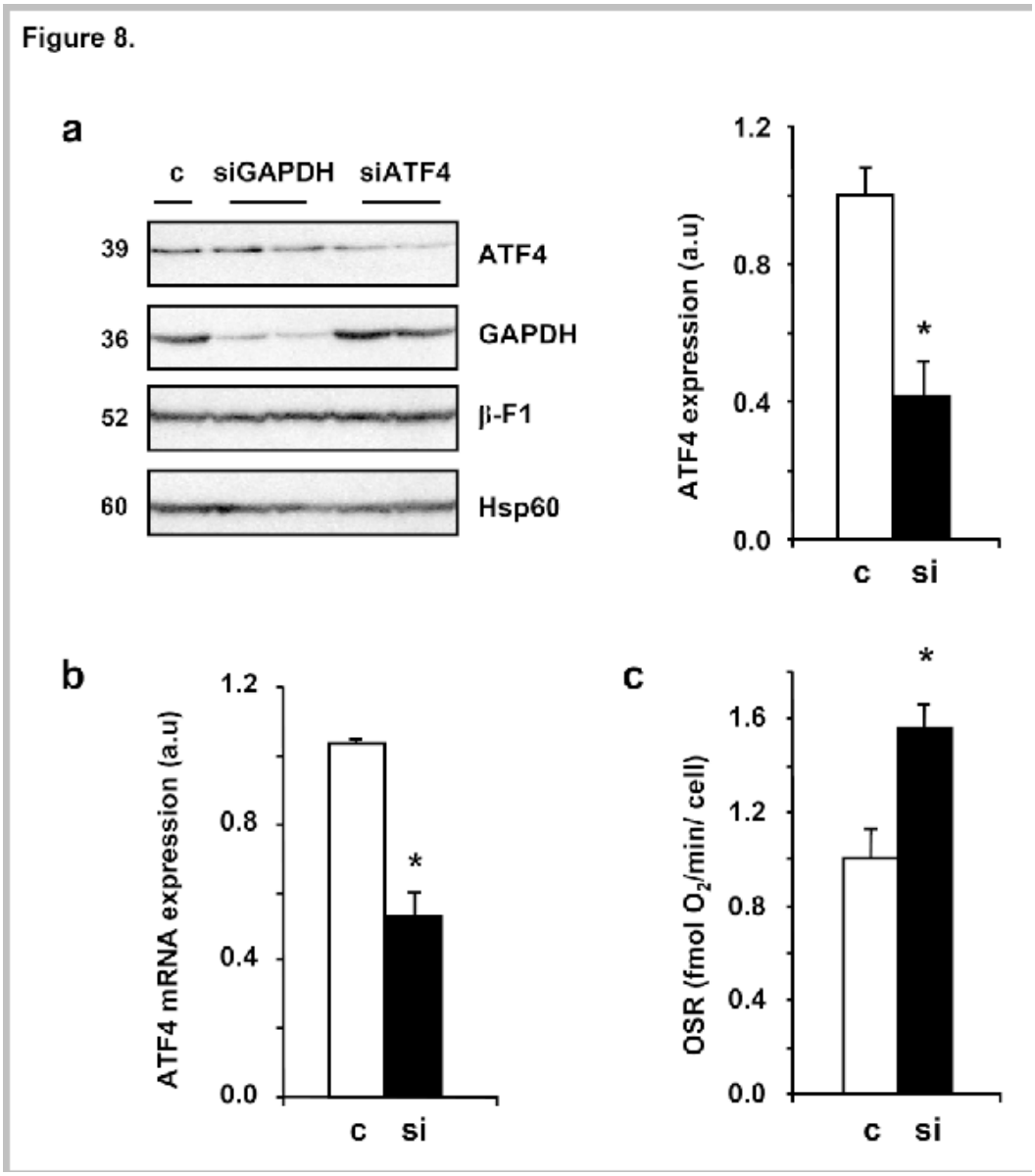

Figure 8. Silencing of ATF4 promotes the bioenergetic function of mitochondria. a, Cellular lysates of control (c), GAPDH-silenced (siGAPDH, also used as control, c) and ATF4-silenced (siATF4) cells were analyzed by western blotting for the expression of β-F1-ATPase (β-F1), Hsp60, GAPDH and ATF4. The histograms show the quantification of the bands normalized to the mean value in control cells. **b,** Cellular mRNA was extracted from control and ATF4-silenced cells and ATF4 mRNA determined by qPCR. **c,** Silencing of ATF4 mediates a large increase in OL-sensitive (OSR) respiratory rate when compared to control cells. The results shown are the mean ±SEM of three (b) or five (c) experiments.* $P < 0.05$ when compared to control cells by Student's *t*-test. The molecular mass of each protein is indicated on the left hand side of the blot.

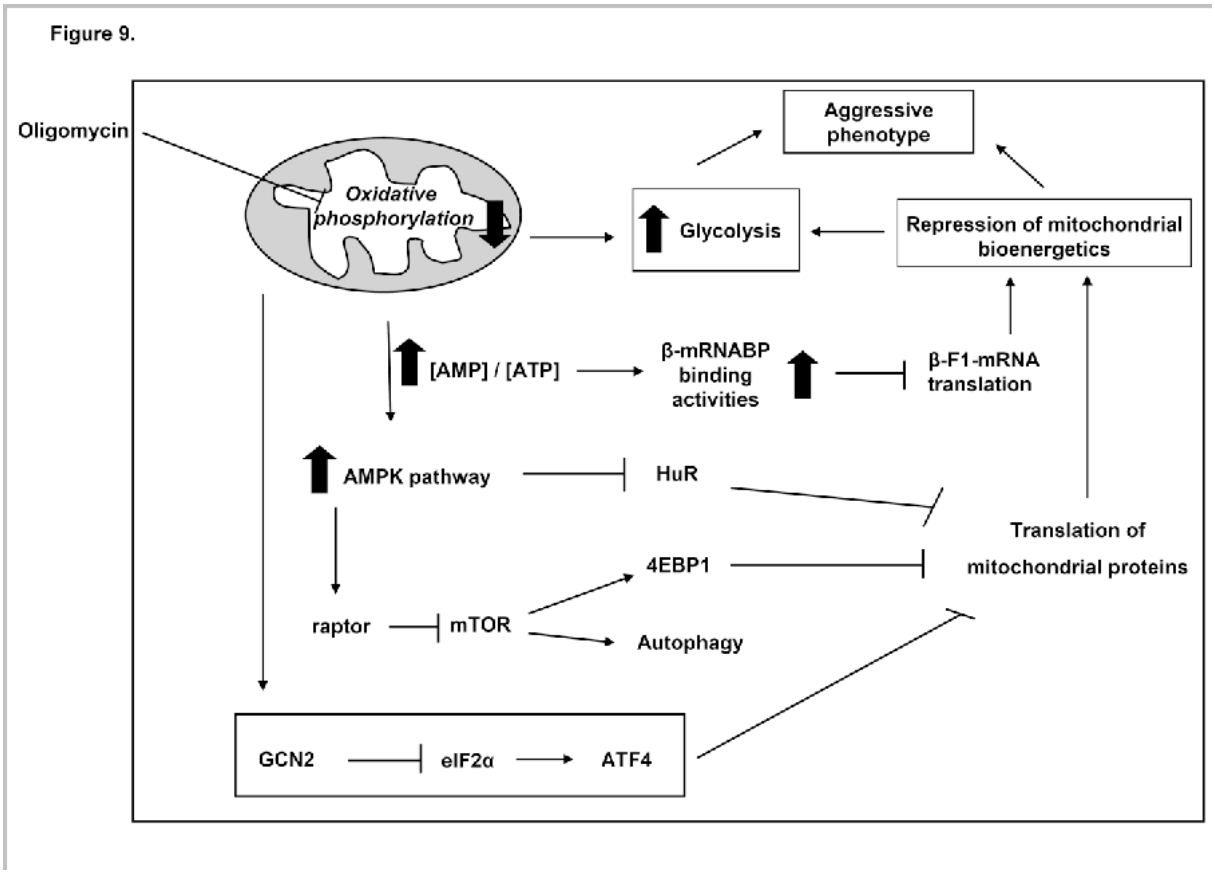

Figure 9. Schematic diagram illustrating the major signaling pathways and mediators involved in the acquisition of the tumor-promoting phenotype in colon cancer cells. Energetic stress triggered by the inhibition of oxidative phosphorylation with oligomycin promotes short-term changes in the AMP/ATP ratio and in the rates of glycolysis. Moreover, OL-treatment promotes the persistent activation of the AMPK and GCN2 pathways. Activation of AMPK, phosphorylates raptor and represses mTOR and HuR expression with further consequences in the augmented expression of 4EBP1 and the induction of autophagy. The activation of GCN2 cooperates with AMPK in down-regulating cap-dependent translation via eIF2α. Overall, all these changes impact at short or long-term on the synthesis of mitochondrial proteins, specifically on β-F1-ATPase synthesis. As a consequence, mitochondrial activity is repressed, enhancing glycolysis and the acquisition of the tumor-promoting phenotype of colon cancer cells.